

# A System for the Analysis and Comparison of Oceanographic Data from Satellite-Borne and in-situ Sensors

M. D. Milnes and J. Keeling

*Phil. Trans. R. Soc. Lond. A* 1988 **324**, 347-363

doi: 10.1098/rsta.1988.0024

## Email alerting service

Receive free email alerts when new articles cite this article - sign up in the box at the top right-hand corner of the article or click [here](#)

To subscribe to *Phil. Trans. R. Soc. Lond. A* go to: <http://rsta.royalsocietypublishing.org/subscriptions>

## A system for the analysis and comparison of oceanographic data from satellite-borne and *in-situ* sensors

BY M. D. MILNES<sup>1</sup> AND J. KEELING<sup>2</sup>

<sup>1</sup> *Logica Space and Defence Systems Ltd, Cobham, Surrey KT11 3LX, U.K.*

<sup>2</sup> *Admiralty Research Establishment, Portland, Dorset DT5 2J5, U.K.*

[Plate 1]

ODESSA is an Oceanographic Database and Environmental Satellite System Application developed for ARE (Portland) by Logica Space and Defence Systems Limited, under Ministry of Defence contract.

It is possible to access online or historic satellite images, which may be processed and displayed in a variety of formats. The oceanographic database contains data as a function of depth that have been derived from a wide range of instruments, geographic areas and times. This database may be accessed and the data processed and displayed in a number of ways, some of which can be directly overlaid and compared with the processed satellite images.

The system was designed to be flexible, with an emphasis on the man-machine interface, making extensive use of menus and graphic input devices. The flexibility allows for easy expansion to include further processing and display facilities.

Examples of output displays are presented to show the application of the ODESSA system in oceanographic modelling studies and in relating sea-surface temperatures to the three-dimensional water-column structure.

### PART I. SYSTEM OVERVIEW

#### 1. INTRODUCTION

An important area in the field of remote sensing is the interpretation of images. It is possible to analyse satellite images individually, in isolation; however, more useful information can be obtained by making use of additional data. These data could be taken from earlier remote observations of the same location, or from *in situ* data, obtained by more conventional means.

The ODESSA system provides the facilities to enable such additional information to be used. In particular, the current *in situ* data set consists of oceanographic data. This requires a considerable amount of processing of satellite images and of oceanographic data before meaningful comparisons between the two data sets can be made.

It is this processing that is described below, from the origins of the algorithms, through the design, to the implementation of the system.

Following this description, and a review of the future potential uses, a specific example of the current application at the Admiralty Research Establishment will be presented.

## 2. BACKGROUND

The system is based on algorithms obtained from the NATO Oceanographic Research Centre (SACLANTCEN) at La Spezia, Italy. These algorithms were developed over a number of years, from 1974 onwards. However, there have been many changes and additions since then, some of which were based on work done for ARE by Logica, investigating the feasibility of the use of infrared satellite images for detecting various oceanographic features, an area of considerable interest in recent years (Robinson 1985). Following this study, ARE placed a contract with Logica to provide a facility for the continuation of this research, and to extend it to include analysis of historical *in situ* oceanographic data.

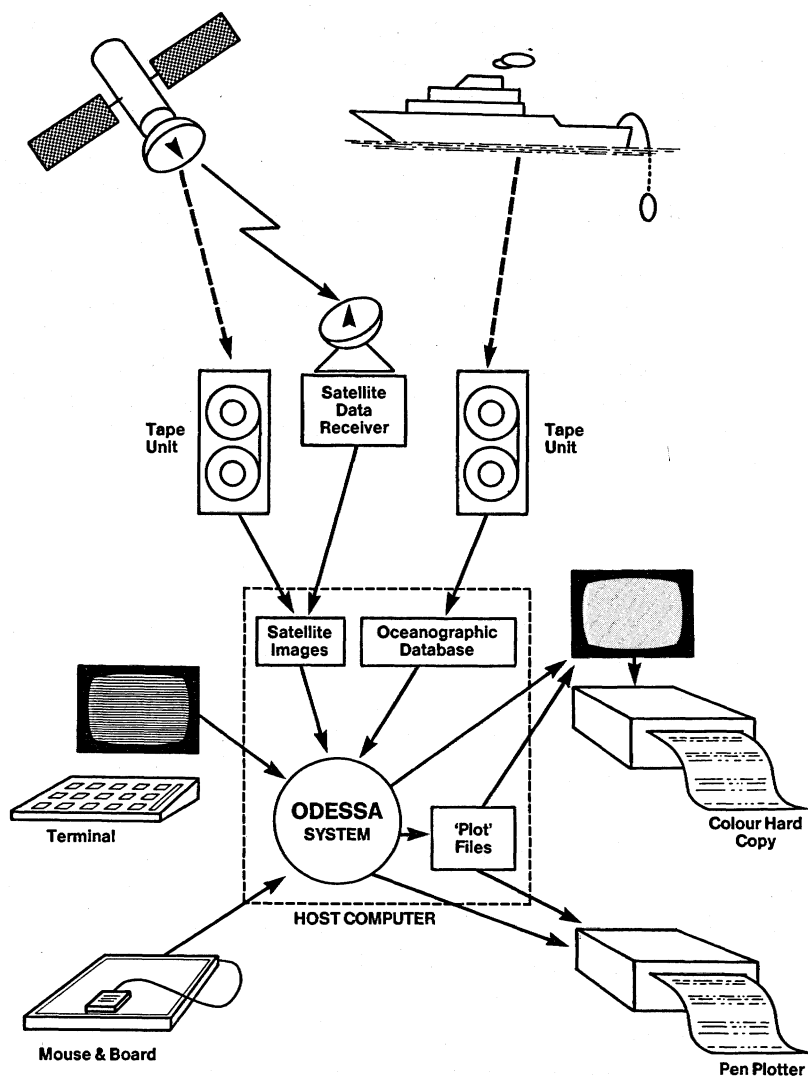


FIGURE 1. The major interfaces and components of the ODESSA system.

### 3. REQUIREMENTS

The requirement was for the implementation of an environmental database, with the ability to relate information from the database to information obtained from remotely sensed infrared images. Figure 1 shows the major interfaces and components of the required system. It was required that the system should handle data from a variety of sources.

(i) Satellite images, obtained from the NOAA series of satellites, either on computer-compatible tape or directly (via a serial line) from a low-resolution satellite data receiver.

(ii) Oceanographic data in the form of temperature–salinity–sound-speed as functions of depth, at a large number of locations, covering a wide geographic area (the whole of the North Atlantic), and spanning a long period of time (many years).

(iii) User input via menus and by use of a graphics input device. This was in fact a mouse and board, which could also be used as a digitizer.

The output display formats were largely determined by the vector displays originally produced at SACLANTCEN, with the addition of further display facilities for raster images, and for the comparison of data sets from different sources.

### 4. DESIGN CONSIDERATIONS

The system was designed to be flexible and easy to use. Both of these are important attributes for a research tool, whose uses and users are likely to change with time.

Flexibility was promoted by the use of LUCID, an image processing software kernel (developed by Logica). With LUCID it is possible to construct complex sequences of image manipulations, which can be easily modified or extended. All the software is written in FORTRAN, and consideration was given to the need for a number of separate databases, each accessible by the same set of software, or a single large database split over several areas.

Ease of use was addressed by providing a menu-driven system, with three basic menu types: single choice, multiple choice, and a standard data input and edit menu. These input and edit menus provide default values for all parameters, which the user can change if required. Wherever possible, a graphics input device was used for specification of inputs, applying particularly to the determination of geographic limits on maps.

The special function keys, in addition to the menu applications, were also programmed to allow interactive analysis of the currently displayed image, at any stage of processing.

There were many other factors which were considered in the design of the system. For example, given the research environment within which the system was intended to operate, the level of automation was kept fairly low, allowing the user to control many of the operations interactively. In addition, the emphasis in the design was on flexibility rather than speed; this has allowed the inclusion of a larger number of features than would have been possible if speed of operation was the major consideration.

All these factors needed to be considered within the overall constraints imposed by the project timescales and budget. (There were six months available to produce the system, from initial design through to final delivery.)

## 5. SYSTEM DESCRIPTION

The hardware on which the system was based is summarized as follows:

- DEC VAX computer, as the main host processor;
- high-resolution colour graphics display, and ink-jet printer, for colour dumps of the screen;
- large (up to A1 paper size) pen plotter, for hard copy of vector outputs from the system;
- terminal and keyboard for user-control of the system;
- mouse and board, for control of cursor on the graphics display, and for manual digitization of data;
- satellite data receiver, connected to the host computer by a serial line.

Processing within the system can be broken down into five broad categories. Two involve only the oceanographic data, these being database loading and accessing, and database analysis options. One category is involved with just the satellite data: satellite image processing. The two data sets are related in the comparison facilities between images and database. Finally, within all of the categories are the special function key operations. The functions performed within each of these areas are now described in greater detail.

*(a) Database loading and accessing*

The system currently allows oceanographic data to be input in any one of three standard formats, from magnetic tape, or from disk file. Alternatively, individual data profiles can be input manually with a digitizer.

To optimize data-access times, the profiles are stored according to geographic areas, and instrument types. Once in the database, the data can be accessed in a variety of ways.

(i) By location, specified by the graphics input device to determine the limits of the search area on a map of the whole region, or numerically by specifying the minimum and maximum latitude and longitude, or the search area can be determined by the limits of a specified satellite image. The geographic location of the data can be further refined to a track of selectable width, a circular region, or a rectangular subregion of the current search area.

(ii) By time, including intervals covering time of day, date and year. The time and date of a selected satellite image can also be used as a basis for specifying the temporal limits.

(iii) By data source, including the specific type of instrument used, the particular ship from which the data were gathered, the general data type and the data quality.

Having identified the data required in this way, the next stage is to analyse the data.

*(b) Database analysis options*

There are five main database analysis options:

- horizontal sections, consisting of plots of the geographic distribution of data;
- vertical sections, showing the variation of a specified parameter along a particular track, plotted against depth;
- profile plots, showing the data as they are stored in the database, as parameter against depth, from particular profiles;
- temperature against salinity plots, with the distribution of the selected data points displayed;
- extraction of inputs to acoustic propagation loss models.

The geographic distribution display allows for various different representations of the data,

including scatter plots (with or without associated values), and contours of selectable interval, width and colour. The data displayed can be temperature, salinity, soundspeed or depth at a fixed level of any other of these parameters. (Thus one can display, for example, isotherms at a particular depth, or the depths of a particular isotherm.) To assist in the location of the data, they can be represented on a choice of map projections, with coastlines, gridlines, and detailed chart borders.

The vertical section display has the same choice of data representation options as the horizontal section. In addition, the sea-bed topography can be simultaneously displayed.

The graphical representations have the option of automatic scaling of axes to fit the available data, or the axis limits can be user-specified.

Likewise, the inputs to the propagation-loss models can be specified in detail by the user, or typical default values can be used.

### (c) *Satellite-image processing*

There are several stages in the processing of satellite images before they can be used for comparison with the oceanographic data extracted from the database. These stages are summarized below.

#### (i) *Image extraction*

This involves reading the image data from magnetic tape, or over a serial line, separating the image from the calibration data stored with each image line, and saving the multiband image on disk.

#### (ii) *Atmospheric correction*

This involves converting the satellite-observed radiance at different frequencies to observed temperatures, by using on-board blackbody calibration data. This conversion is performed by the algorithms recommended by NOAA (1979). The observed temperatures are then converted to estimated sea-surface temperatures by making allowance for atmospheric absorption and attenuation. There is now a choice of a dozen different atmospheric correction algorithms, each relying on the linear combination of observed temperatures in different frequency bands. These algorithms were derived from a number of sources (e.g. Bernstein 1982).

In addition, new algorithms can be easily introduced, if required. From this point onwards, the satellite image is stored as a 'temperature image', with pixel values calibrated in tenths of kelvins.

#### (iii) *Geometric correction*

The space view of earth needs to be converted to a standard map projection to allow direct comparison with the oceanographic data. This is achieved by modelling the orbit of the satellite, and the Earth-satellite geometry. To produce a useful model, the user is required to specify various orbital parameters, and to specify the required location, size, scale and projection of the corrected image. The limits of the corrected image are then displayed on the uncorrected image as an appropriately distorted polygon. To obtain accurate location of the transformed image, the coastline overlay can be used as a 'ground control point', by aligning the overlay with those visible portions of coastline on the image.

The image is now in a state where comparisons with oceanographic data can be made.

However, there are various further enhancements which can be applied to the satellite image, if required. These include:

- identification of cloud, creation of a cloud overlay, and limited interpolation beneath clouds (to provide an estimate of sea-surface temperatures under cloud-affected areas); further work is still required in this area, however, useful results can already be obtained (Gower 1985);

- coastline, landmass, bathymetry overlays;

- the ability to combine cloud and land overlays to give a composite image with land represented black, cloud white, and the visible sea-surface various shades of grey or coloured according to a user-controlled temperature scale;

- a range of image-processing facilities such as median filtering, edge enhancement and contouring;

- extraction and display of observed sea-surface temperature (SST) along a selected track.

(d) *Comparison facilities between images and database*

The main comparison facility available is the ability to display satellite images to the same scale and projection, and covering the same geographic areas as the output from the database analysis software. Figure 2 provides a representation of this facility, which is a key component of the ODESSA system.

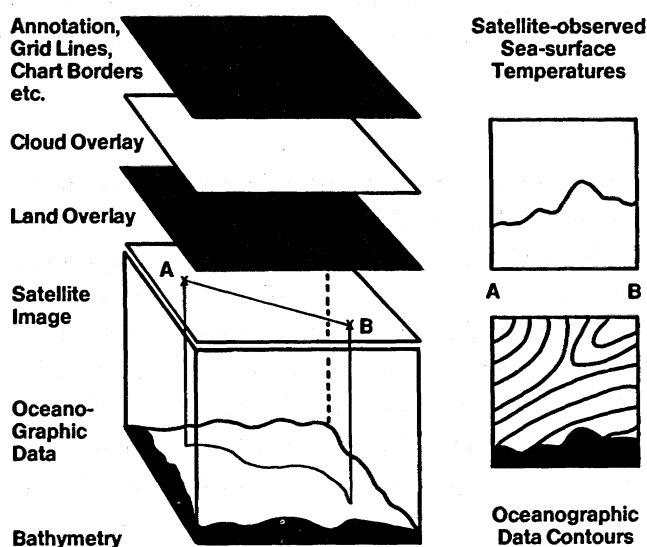


FIGURE 2. Relations between the various data sets and displays in the ODESSA system.

It is also useful to be able to display data from different sources in the same format, so the system allows the oceanographic data to be displayed as a raster image, with the same colour coding as the satellite image.

Alternatively, the satellite image can be contoured, and related to the contour output from the database analysis suite.

In addition, it is possible to show the limits of satellite images overlapping the current search area, and the overlapping portions of those images.

Any vector output can be put on the overlay plane, and superimposed on any raster image.

Furthermore, any vector output can be saved in a device-independent 'plot file' for later display via the colour monitor, pen-plotter, or graphics terminal.

The screen can be split into four sections, and separate displays put in each quarter, to allow for direct comparisons on a single screen.

As a further aid to interpretation of the images, the bathymetry of the specified region can be displayed as an image, with depth scale. Alternatively depth contours can be produced, and overlaid, if required.

The sea-depth information obtained from the bathymetry data is combined with the sound-speed profiles derived from the database for use in the input to the propagation-loss models. The track selected for display of a vertical section (along track against depth) can also be used directly, to extract the sea-surface temperature from a satellite image. Statistical analysis of direct comparisons between database-derived information and satellite-image-derived data can be made, and graphical representation of these can be displayed.

#### (e) *Special function key operations*

Operations using special function keys are available at almost any stage of processing within the ODESSA system. They allow interactive display manipulation, including stretching grey-scales and setting false colours, pan and zoom, screen annotation, and screen deletion.

In addition, when a temperature image is displayed, the temperature at any point in the image can be obtained and a temperature scale added.

Likewise, when a bathymetry image is displayed, depth at any point and a depth scale can be obtained.

### 6. FUTURE DEVELOPMENTS

There are many ways in which this system could be further developed; these include the following.

(a) Extension to include other satellites and data types. Also the data need not be restricted to oceanographic data; any spatially dependent information could be used.

(b) Closer integration of data derived from different sources, for example:

integration of images obtained from different satellites;

use of *in situ* sea-surface temperatures to assist in the interpolation of satellite images beneath cloud;

performance of some form of 'interpolation' between data sets; this includes, for example, temporal 'interpolation' of the same geographic area, to derive information about the surface motion (see, for example, Clark *et al.* 1981; Ninnis *et al.* 1986), and spatial 'interpolation' between data sets at different depths.

In the long term an approach such as this could lead to the ability to produce predictions of the sea temperature at depth, based on sequences of cloud-affected satellite images of the sea surface and historical *in situ* data below the surface.

(c) Develop the user interface further, in particular in the areas of locating ground control points, and of cloud identification, where knowledge-based systems could have a useful role.



## PART II. APPLICATION

A preliminary examination of data gathered during a survey of the Iceland–Faeroes region with the ODESSA system.

## 7. DATA DESCRIPTION

The application of satellite remote sensing to oceanography is of great importance to the Ocean Science Division at the ARE, U.K., with particular emphasis on the task of applying remote-sensing techniques in support of acoustic propagation studies. ODESSA was used in an investigation of the main oceanographic features of the Iceland–Faeroes region, in particular, the Iceland–Faeroes front, which forms the northeastern boundary of the Atlantic Ocean. It is created by the meeting of the cold waters of the Norwegian Sea in the north with the warmer, more saline waters of the North Atlantic Ocean. The frontal position is fixed by the underlying bathymetry where a broad ridge of less than 500 m depth stretches from the Icelandic Continental shelf to the Faeroe Islands.

For many years this region has been the subject of a number of investigations (see, for example, Dietrich 1967), following the discovery of an overflow of cold Norwegian water that spills over the ridge and spreads south to form part of the Atlantic Deep Water Body (Worthington 1976). Figure 3 shows the characteristics of the front with its location in the upper 25 m. The front extends from approximately 64° N at an angle of about 40° with the Iceland–Faeroe ridge, its apex being on the Icelandic continental shelf. In the region of

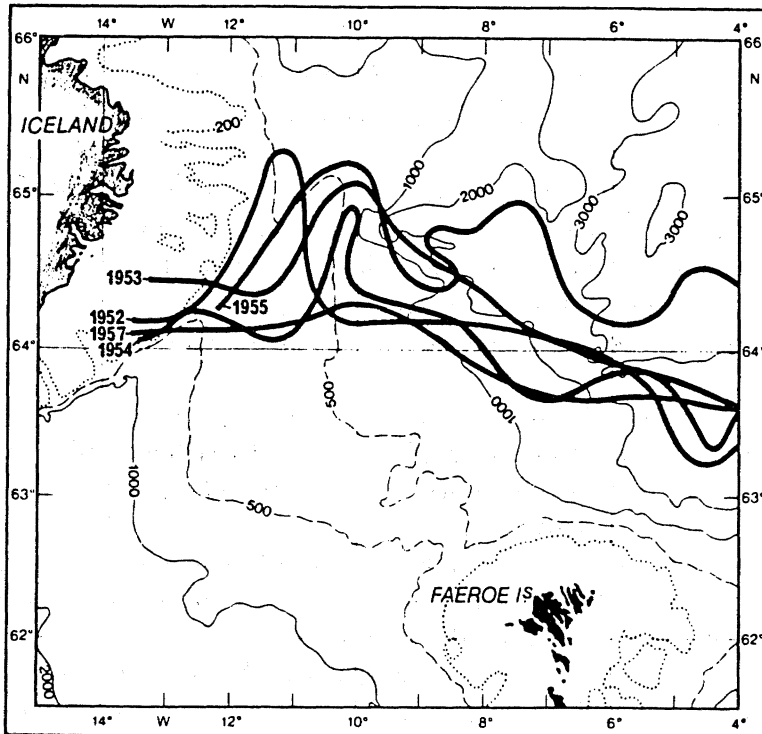


FIGURE 3. Locations of the Iceland–Faeroes front in the surface layer (0–25 m) in May and June of the years 1952 to 1957. The lines correspond to the 35.0 p.p.t. (by mass) isohaline, which represents the zone of maximum horizontal gradients (compiled from *Annls Biol* (1952–1957)).

100–150 km along the front from the Icelandic coastline, at the sea surface, lies an intrusion of warm Atlantic water covering a large area of the sea surface extending northwards into the colder Norwegian Sea water. The frontal area between the intrusion and the Icelandic coast appears to be dominated by eddying and meanders, while the area to the east of the intrusion is ill-defined and further displaced from the Iceland–Faroes ridge, which could be due to the greater amount of mixing in that region or the general increase in depth. Either of these, combined or in part, could be a factor influencing the general trend of the front.

*In situ* sea truth data and infrared satellite images were gathered during a survey of this region from 8–28 June 1986, and provide corroboratory evidence for the frontal position as shown by the satellite images, with the combination of the frontal position from the satellite image and the subsurface hydrography allowing the development of the concept of the front as a three-dimensional feature. The preliminary examination of survey data has made extensive use of the facilities available in the ODESSA system. In particular, the facilities within ODESSA have been used to analyse:

- the spatial and temporal variability of the Iceland–Faeroes Front;
- the effect of bathymetry on the Front;
- temperature differences between remotely sensed and sea truth data.

The distribution of survey measurements is shown in figure 4; the measurements consist of 382 expendable bathythermograph temperature profiles. Several cloud-free and partly cloud-free advanced very-high-resolution radiometer images from the *NOAA-9* satellite were available for the period. The image for 21 June 1986 is displayed in figure 5. A selection of representative temperature against depth profiles are shown in figure 6. In addition, historical data, available within the system, were used to compare with features observed from the survey data and highlighted previously by other workers in this field.

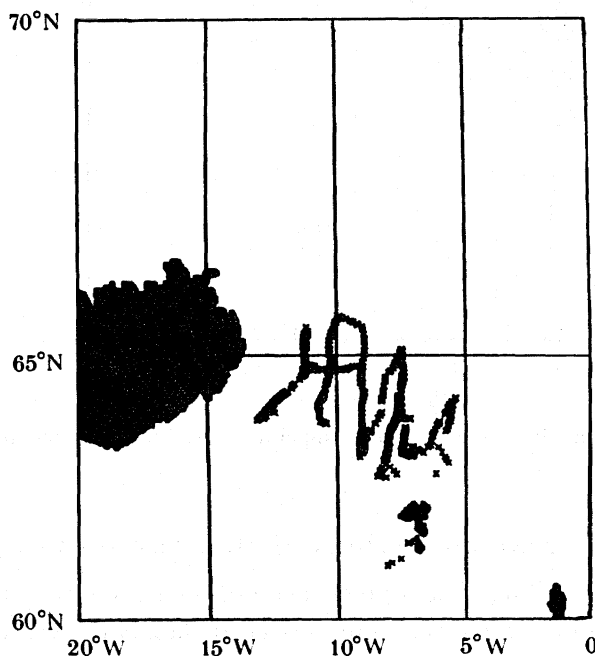


FIGURE 4. Scatter plot of expendable bathythermograph profiles gathered during a survey of the Iceland–Faeroes region in June 1986.

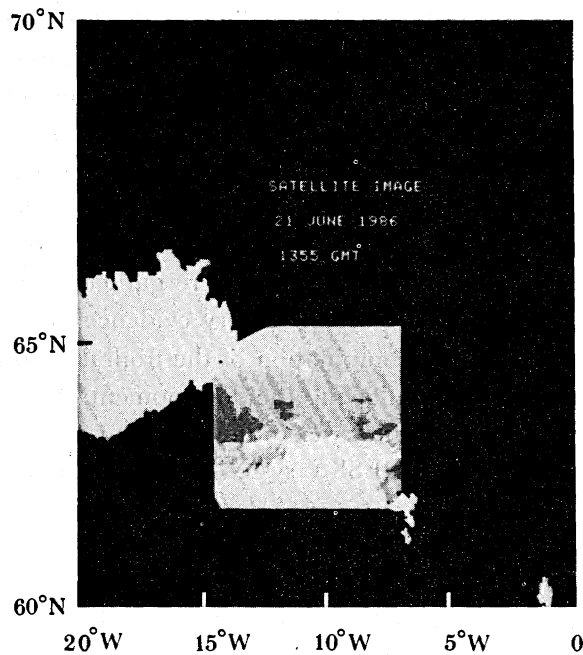


FIGURE 5. Geographical location of a satellite subimage for 13 h 34 GMT 21 June 1986, with the upper-left and lower-right corners impinging on the coastlines of Iceland and the Faeroes respectively.

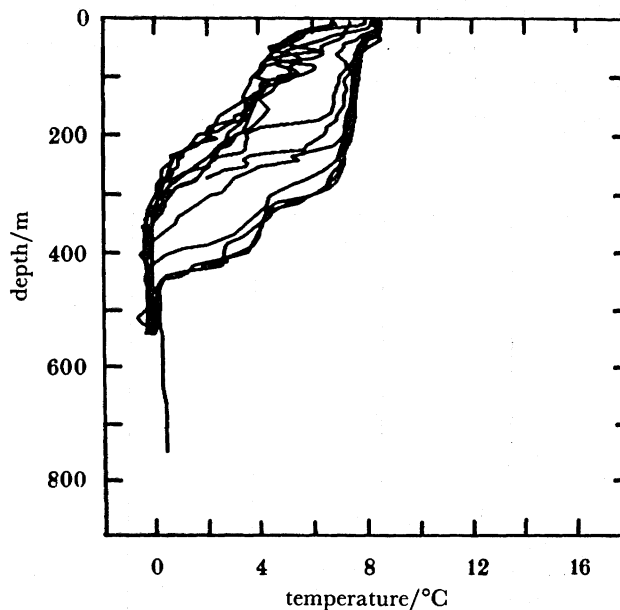


FIGURE 6. Expendable bathythermograph temperature profiles as a function of depth.

#### 8. METEOROLOGICAL CONDITIONS DURING THE SURVEY PERIOD

An examination of the prevailing meteorological conditions during the survey period showed an anticyclonic pattern with light winds and mainly clear skies with occasional fog. However, a period at the beginning of June and in the middle of the survey period produced cyclonic conditions with deep depressions forming to the west of Iceland producing fresh to strong southwesterly winds in the Iceland–Faeroes region.

## 9. SATELLITE IMAGE ANALYSIS

All cloud-free satellite images for June 1986 were incorporated into the ODESSA satellite image directory. The subimage for 21 June (figure 7), presented in Mercator projection, shows a sea-surface-temperature representation of the area, with the warm Atlantic water dominating the central upper part of the image and the colder Norwegian Sea water to the north. The image has been processed and enhanced to show the frontal area with associated eddies and

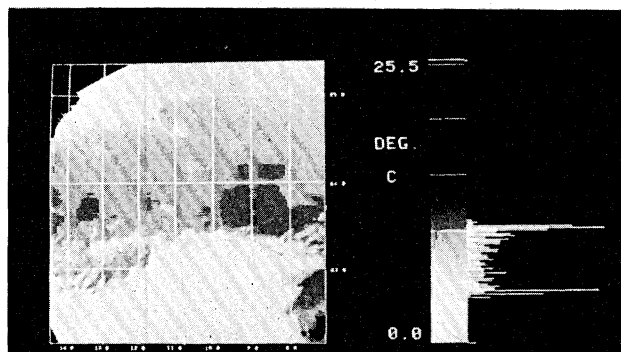


FIGURE 7. NOAA-9 high-resolution subimage, obtained from Dundee University, atmospherically and geographically corrected and shown here in Mercator projection as a 'temperature' image; i.e. each pixel represents absolute values of sea-surface temperature as shown on scale. Image, T392W; location, S.E. Iceland front; date, 21.06.86; time, 13h34; satellite, N9.

a well pronounced cyclonic hook protruding from the western side of the warm intrusion evident in the upper central part of the subimage. Other satellite images for the period portray the hook in various stages of decay and development suggesting a fairly brief life cycle, though the lack of images in sequence prevent conclusions being drawn regarding the period of this feature.

Another interesting feature is the cold eddy in the centre of the subimage at approximately  $64.3^{\circ}$  N,  $10.5^{\circ}$  W. Earlier images seem to indicate that the formation of the eddy may be due to a cold tongue of Norwegian Sea water intruding across the unstable frontal interface into the warmer Atlantic water and subsequently being cut off by the warm water of the cyclonic hook feature overriding the cold dense water of the intrusion. An investigation of this feature with *in situ* data corresponding to a track through the eddy, indicates a modified surface temperature structure with stronger temperature gradients at depth. The structure and behaviour of the front and associated mesoscale features have been the subject of many studies (see, for example, Willebrand & Meincke 1980; Smart 1984).

Meincke (1975) indicated that the eddy generation might be linked to changes in the atmospheric pressure distribution. However, Willebrand & Meincke (1980) indicated that baroclinic instability and the tendency of the mean bottom currents to follow the isobaths, causing eddy-like structures to emanate from the near-bottom layer, were the likely sources of eddy generation and intermittent overflow and only occasionally, during the passage of strong atmospheric cyclones, would forcing be likely to play a dominant role.

## 10. TEMPERATURE COMPARISONS

The relation between the direct measurement of sea surface temperature by shipborne instruments and the infrared-derived measurements of the top millimetre skin layer of the sea-air interface has been tentatively assessed by comparing data obtained along the ship's track with corresponding pixel data on the image. Figure 8 is an example of a case in which

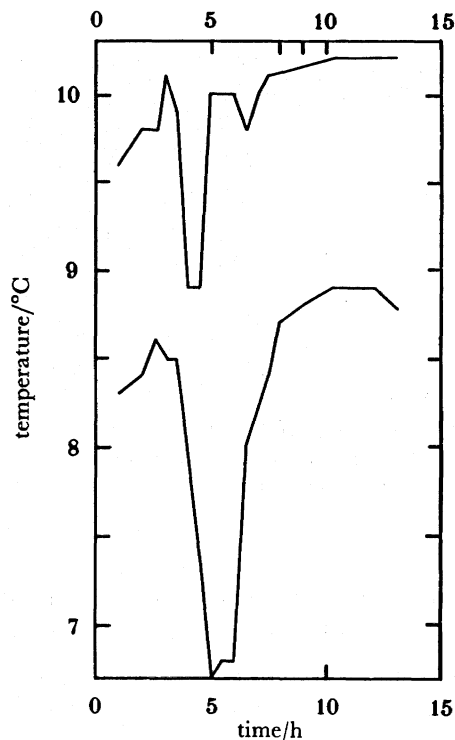


FIGURE 8. The relation between direct measurements of sea surface temperature by shipborne instruments and the infrared-derived measurements may be examined by relating latitude and longitude of *in situ* data with corresponding pixel data on the image. The fairly constant difference evident here may well point to strong solar heating with resultant positive differences between data sets. Upper curve, satellite-derived data, 21h13 min 55 GMT, June 1986; lower curve, *in situ* data, 21 June 1986; RMS difference, 1.86 K.

*in situ* and satellite-derived data may be compared by using the ODESSA system. The *in-situ* temperature data and the corresponding satellite pixel temperature values are plotted against time with the two data sets matched as closely as possible in time, to enable a comparison to be made. The RMS difference between the two sets is 1.86 K; the general trend of the temperature distribution is clearly mirrored in both data sets.

More important to this qualitative account is the relation between the direct measurements of sea surface temperature and the temperature related features depicted by the image. An appraisal of the data presented in two forms: vector and raster mode, enabled comparisons to be made of the contoured data from the satellite image and the raster image generated from the contoured *in situ* data (figure 10). A comparison of the overall grey level distribution in both images reveals the lighter shades in the *in situ* image and, correspondingly, the contoured *in situ* data indicate a lower temperature field with less complex and smoother defined contours

than those in the satellite-derived contours. Generally, however, comparison of the *in situ* data with those derived from the satellite shows similar sized temperature ranges for the water masses and frontal water with the subimage appearing, as in figure 8, 1–2 K warmer. Moreover, meteorological conditions for the period covered by the satellite image were favourable for strong solar heating to produce conditions of positive differences to occur between satellite-derived and *in situ* sea surface temperature, indicating a possible explanation for the warmer 'skin' temperature.

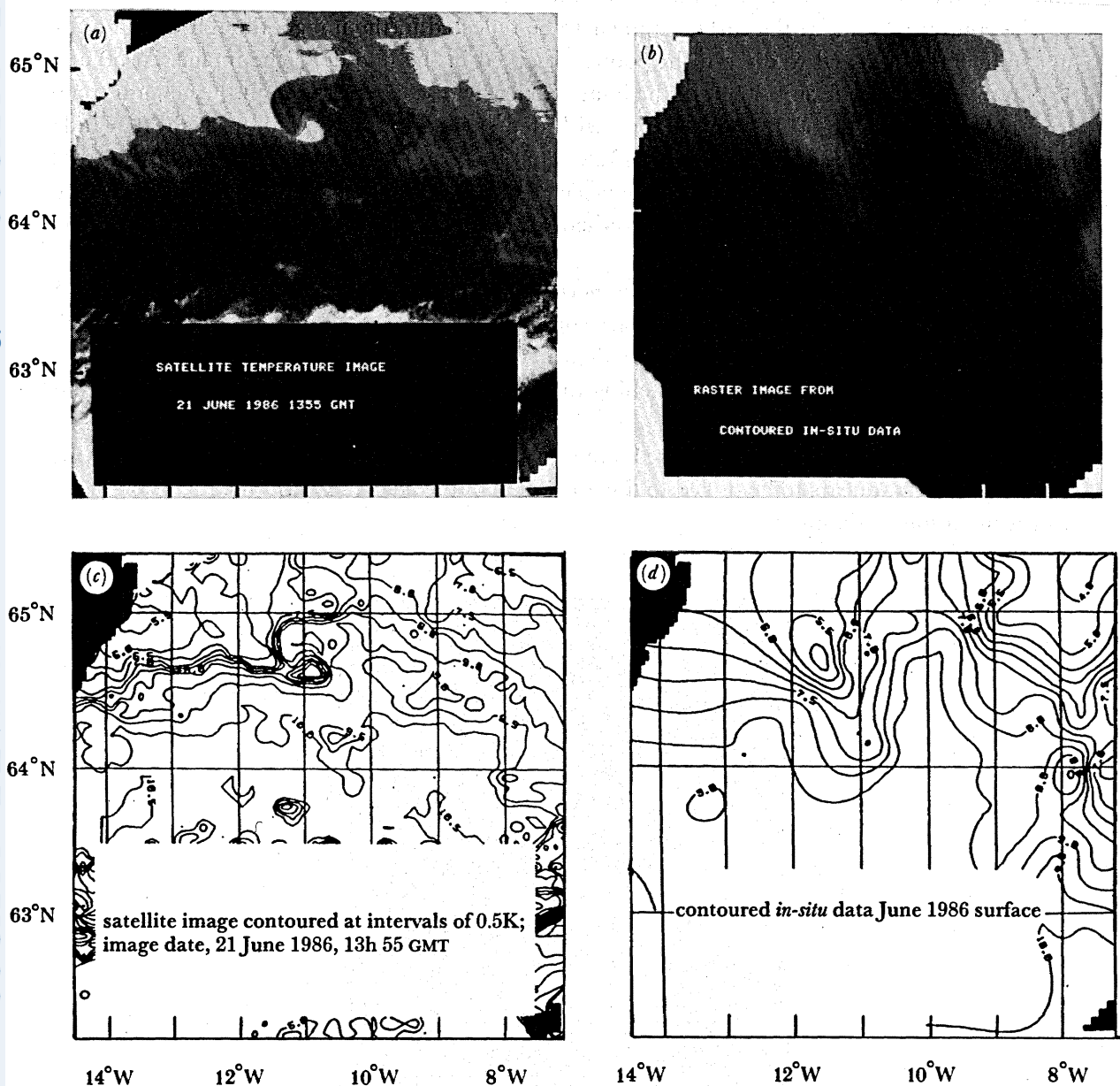


FIGURE 10. Satellite-derived and *in situ* measurements of sea-surface temperature presented in raster and vector mode. Both sets of contoured (vector) data show the general distribution of warm Atlantic water with the cooler Norwegian Sea water to the north. Comparison between overall grey level distribution in both raster images indicate the lighter shades in the *in situ* image corresponding to a lower temperature field.

## 11. INTERCOMPARISON BETWEEN DATA SETS

The satellite subimage, overlaid with *in situ* contoured temperature data, provides information on the vertical structure of the ocean in this region. Figure 9, plate 1, shows data gathered during the period 8–28 June 1986 representing the data set to correspond with the 21 June image. An initial study of the satellite images available for this period indicated no significant change in the location and general shape of the frontal feature. The combining of *in situ* data over this timescale enabled the approximate location and shape of the front to be determined, allowing study of the underlying water column.

The contoured data at the surface appear to be reflected in the image, though the data are not sufficiently resolved to discern the eddies observed in the middle of the image. At 50 and 180 m the warm intrusion evident in the image is clearly discernable, though the general trend is a southward incline of the frontal zone with depth. This spatial variation of the Iceland–Faeroes front was studied by Smart (1984). Smart concludes that the location of the front can be displaced by as much as 150 km between 50 and 350 m depth. The overall displacement of the zone of maximum temperature gradient observed in figure 9 is not as apparent as in the observations of Smart.

An interesting feature is the well pronounced meandering of the front, which presents an S shape at 180 through 350 m depth. Smart commented on this S shape, observed during his appraisal of the frontal displacement at depth, though his observation was of a recurring inverted S-shaped meander closely matching the 500 m depth contour at the southwestern edge of the Iceland–Faeroes ridge.

Though the feature evident in figure 9 may be topographically driven, the strong recurving to the northeast appears to be linked to the formation of the cold eddy and the inversion of the warm intrusion at depth.

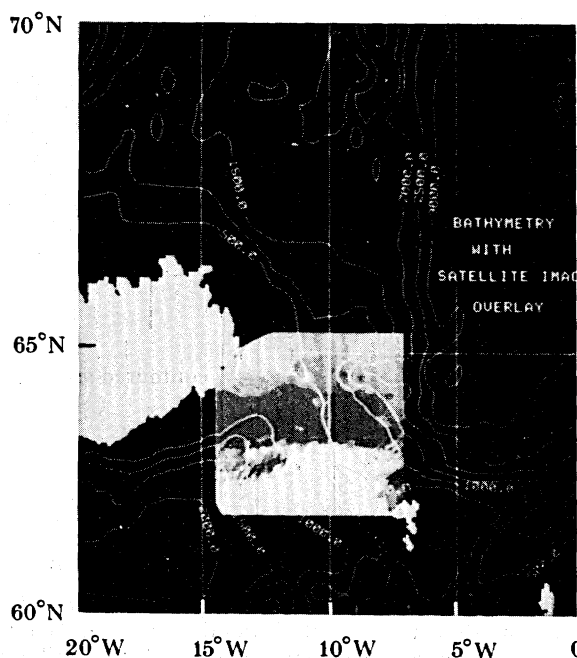


FIGURE 11. Satellite subimage overlaid on bathymetry contours. The spacing of the contours may be selected interactively by the user.



FIGURE 9. Contoured *in-situ* temperature data at significant depths of near-surface, 50m, 180m and 350m depth overlaid on the satellite subimage; an example of how *in-situ* data can be compared with accurately registered and atmospherically corrected satellite images.



Figure 11 shows the bathymetric contours in the area covered by the satellite subimage. The correlation between the surface and the bottom structure is small though the warm intrusion follows the northward extent of the Iceland–Faeroes ridge. However, the zone of maximum temperature gradient evident in all the contoured data in figure 9 at approximately  $64.5^{\circ}\text{N}$ ,  $12.0^{\circ}\text{W}$  correlates well with the bathymetric contours associated with the South Iceland Channel. Moreover, the frontal feature appears to follow the 500 m contour at 350 m depth, an observation also made by Smart, though the northeastern edge of the front appears to follow the northern boundary of the Iceland–Faeroes ridge.

## 12. VERTICAL SECTION THROUGH THE FRONTAL ZONE

A section was taken through the frontal zone corresponding to a track of the survey vessel. Figure 12 shows temperature contours generated from the *in situ* data along the ship's track and exposes the slant of the front showing clearly the outflow of cold Norwegian Sea water spilling

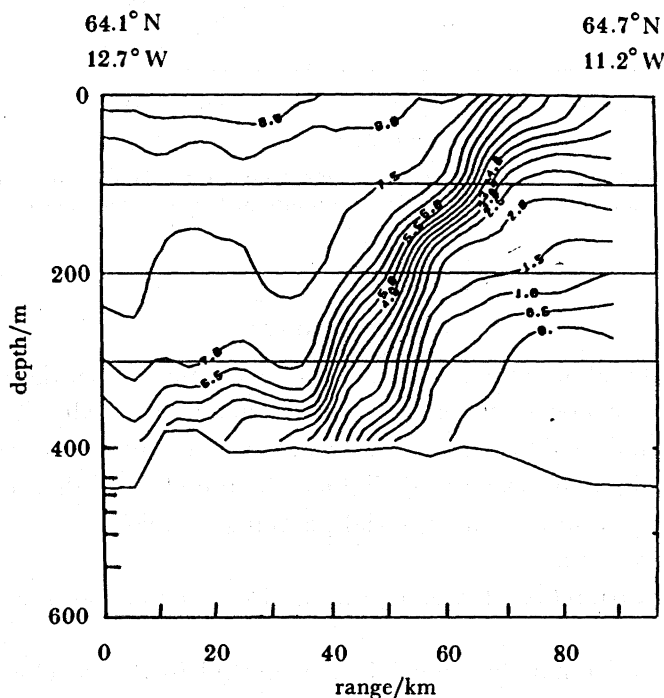


FIGURE 12. Temperature section along the crest of the Iceland–Faeroes ridge, obtained by the survey vessel in the period 22–23 June 1986.

over the ridge with the warm Atlantic water to the south. The surface expression of the frontal zone correlates well with the satellite image indicating the zone of maximum temperature gradient. Additionally, the ODESSA system allows the creation of data files for input into propagation loss models. Figure 13 shows selected sound velocity profiles produced from the track temperature data (figure 12) and subsequent output, showing the effect of the oceanography on the propagation of sound with a large transmission loss through the frontal zone.

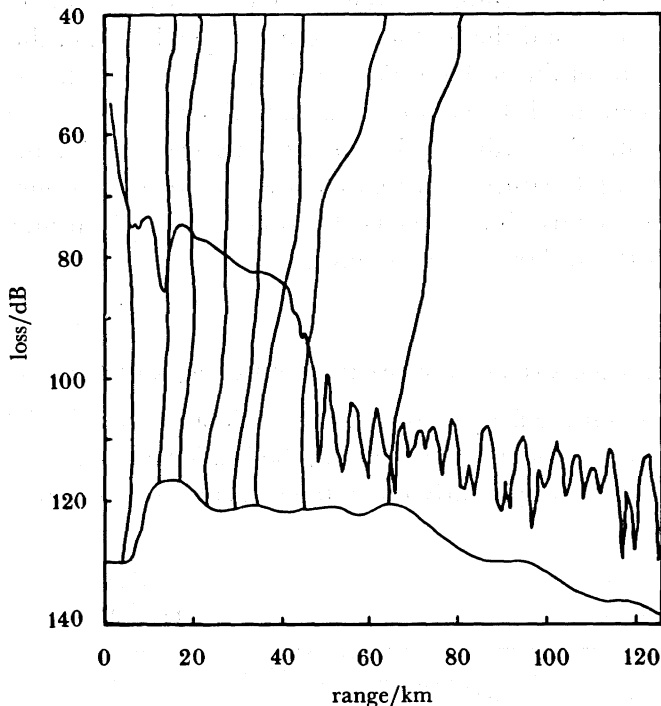


FIGURE 13. Series of sound velocity profiles generated from track temperature data (figure 12) and output from a parabolic equation propagation loss model showing transmission loss as a function of range, with bottom topography superimposed.

### 13. CONCLUSIONS

The initial analysis of the data obtained during the survey has shown the relative ease with which large amounts of oceanographic *in situ* and corresponding satellite image data can be processed, manipulated and analysed by the ODESSA system within very short timescales.

The preliminary investigation has also highlighted the use of ODESSA for the following.

(a) Oceanographic area appraisals for pretrial planning exercises.

(b) Oceanographic analysis of:

spatial and temporal variability of oceanographic features (temperature, salinity, sound speed);

comparison of *in situ* and remotely sensed data as an aid in the development of satellite atmospheric correction algorithms;

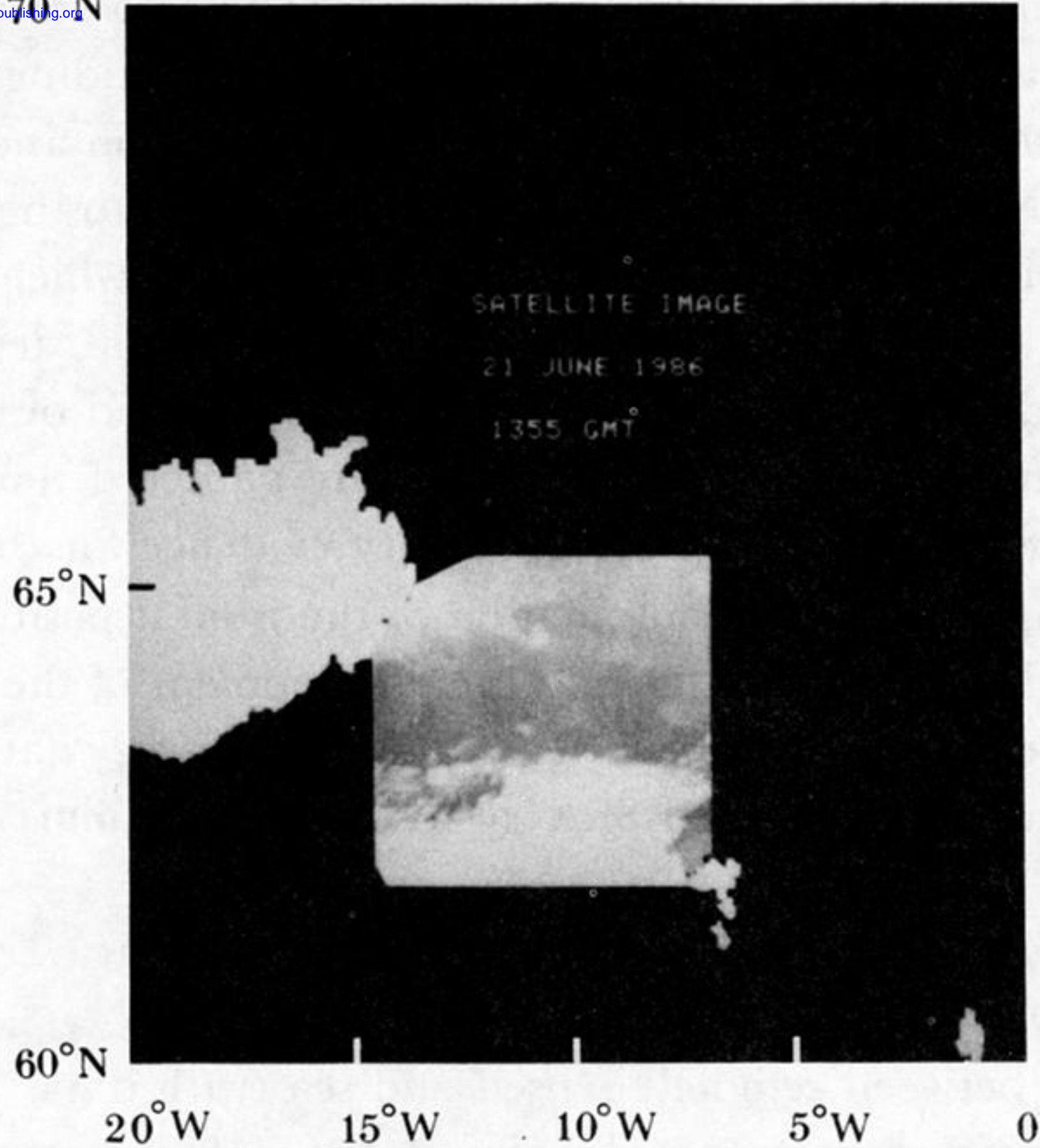
(c) deriving water-column structure from satellite infrared images and *in situ* data as an aid in oceanographic modelling and acoustic propagation studies.

In conclusion, the ODESSA system represents a step in the future direction of the application of remotely sensed data, in that it involves integration with data from other sources. It is a research tool which has considerable potential for further development in the integration and analysis of remotely sensed images with *in situ* data.

## REFERENCES

- Bernstein, R. L. 1982 Sea surface temperature estimation using the NOAA-6 satellite AVHRR. *J. geophys. Res.* **87**, 9455–9465.
- Clark, J. R. & LaViolette, P. E. 1981 Detecting the movement of oceanic fronts using registered *Tiros-N* imagery. *Geophys. Res. Lett.* **8** (3), 229–232.
- Dietrich, G. 1967 In *Review of the international 'overflow' expedition (ICES) of the Iceland–Faeroe Ridge, May–June 1960* (CPI Pour L'Exploration de la Mer. Rapports et Proces verbaux, vol 157), pp. 268–274.
- Gower, J. F. 1985 Reduction of the Effect of Clouds. *J. Remote Sensing* **6** (8), 1419–1434.
- Meincke, J. 1975 Overflow 73 – evidence for atmospheric forcing of Arctic water events. ICES Hydrogr. Comm. CM 1975/C: 29.
- Ninnis, R. M., Emery, W. J. & Collins, M. J. 1986 Automated extraction of pack ice motion from AVHRR imagery. *J. geophys. Res.* **91** (C9), 10725–10734.
- NOAA 1979 Data Extraction and Calibration of TIROS-N/NOAA Radiometers. Technical memorandum NESS 107. Washington, D.C.: Department of Commerce.
- Robinson, I. S. 1985 *Satellite oceanography*. Chichester: Ellis Horwood Ltd.
- Smart, J. H. 1984 Spatial variability of the major frontal systems in the North Atlantic–Norwegian Sea, 1980–81. *J. phys. Oceanogr.* **14**, 185–197.
- Willebrand, J. & Meincke, J. 1980 Statistical analysis of fluctuations in the Iceland–Scotland frontal zone. *Deep Sea Res.* **27A**, 1047–1066.
- Worthington, L. V. 1976 *On the North Atlantic Circulation*. Baltimore and London: The Johns Hopkins University Press.

70°N



65°N

60°N

20°W

15°W

10°W

5°W

0

FIGURE 5. Geographical location of a satellite subimage for 13 h 34 GMT 21 June 1986, with the upper-left and lower-right corners impinging on the coastlines of Iceland and the Faeroes respectively.

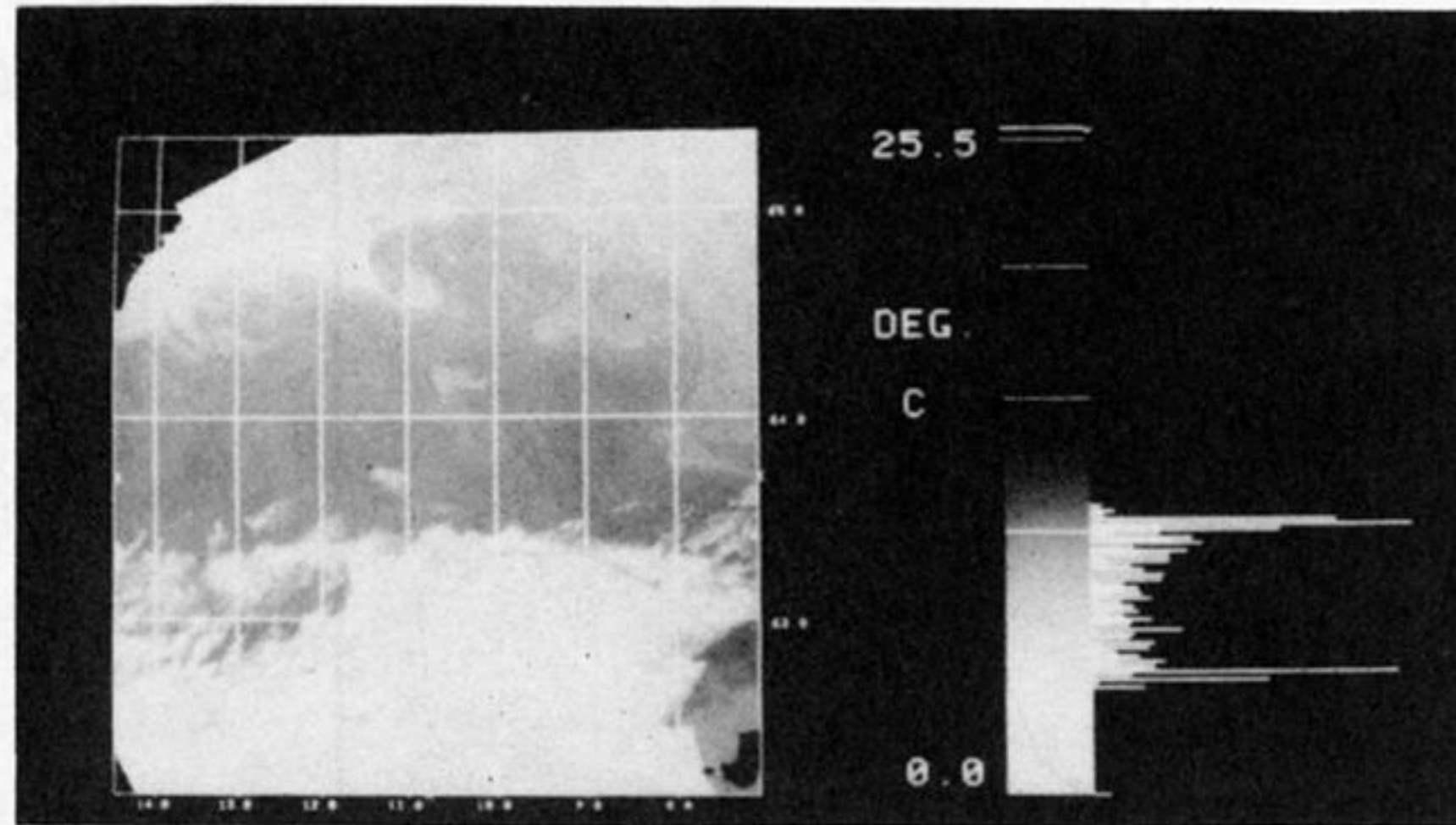


FIGURE 7. *NOAA-9* high-resolution subimage, obtained from Dundee University, atmospherically and geographically corrected and shown here in Mercator projection as a 'temperature' image; i.e. each pixel represents absolute values of sea-surface temperature as shown on scale. Image, T392W; location, S.E. Iceland front; date, 21.06.86; time, 13h34; satellite, N9.

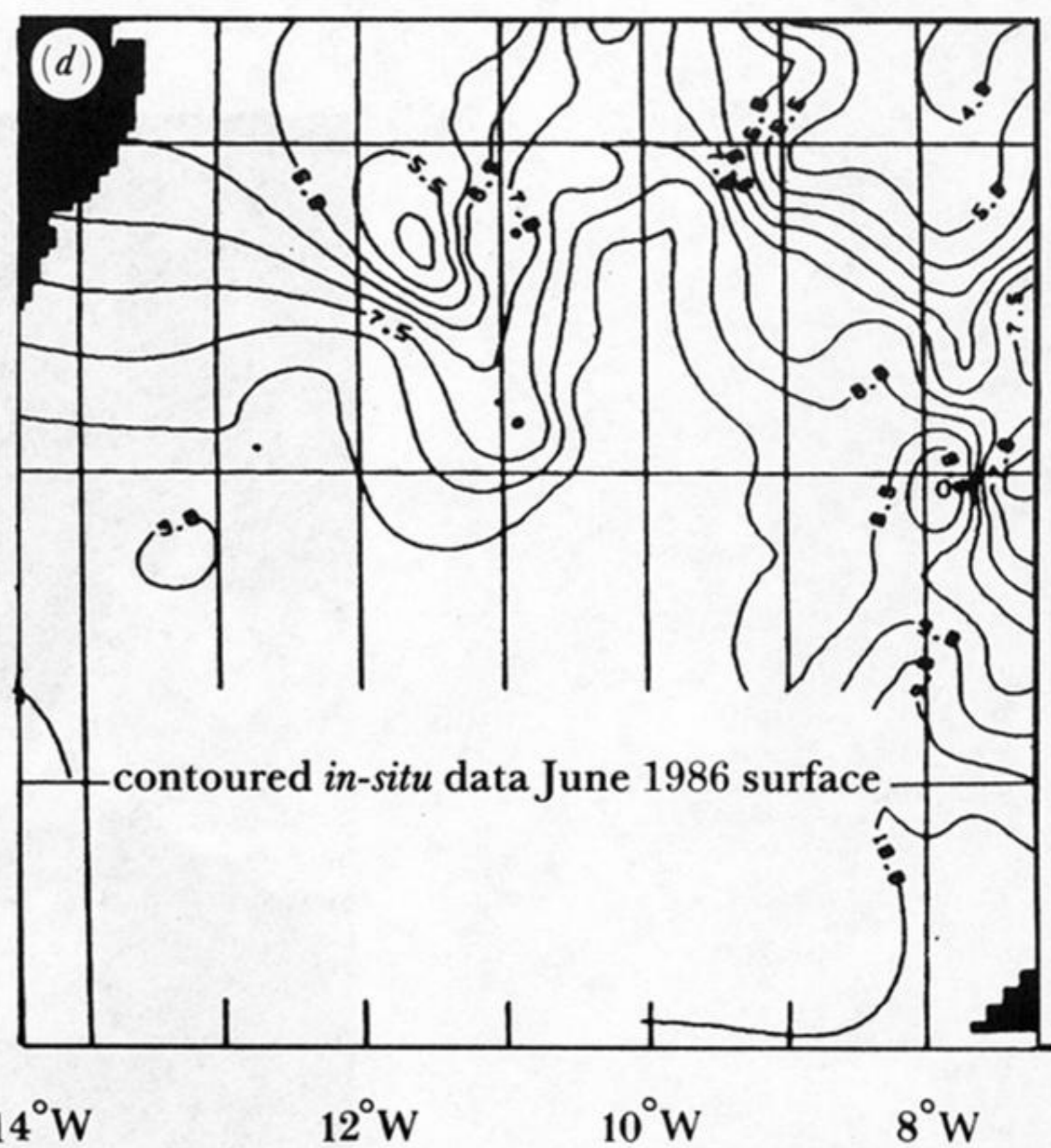
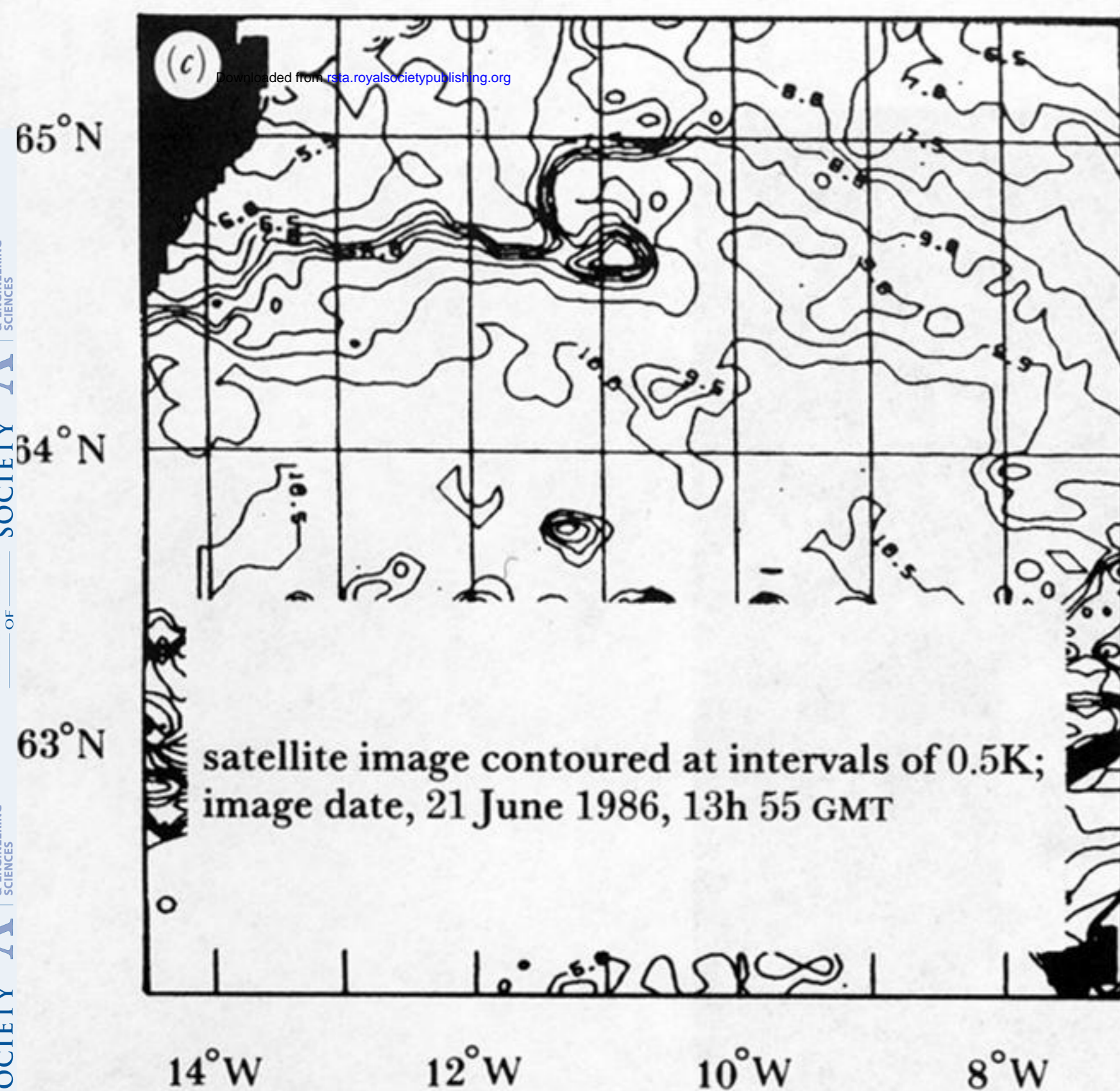
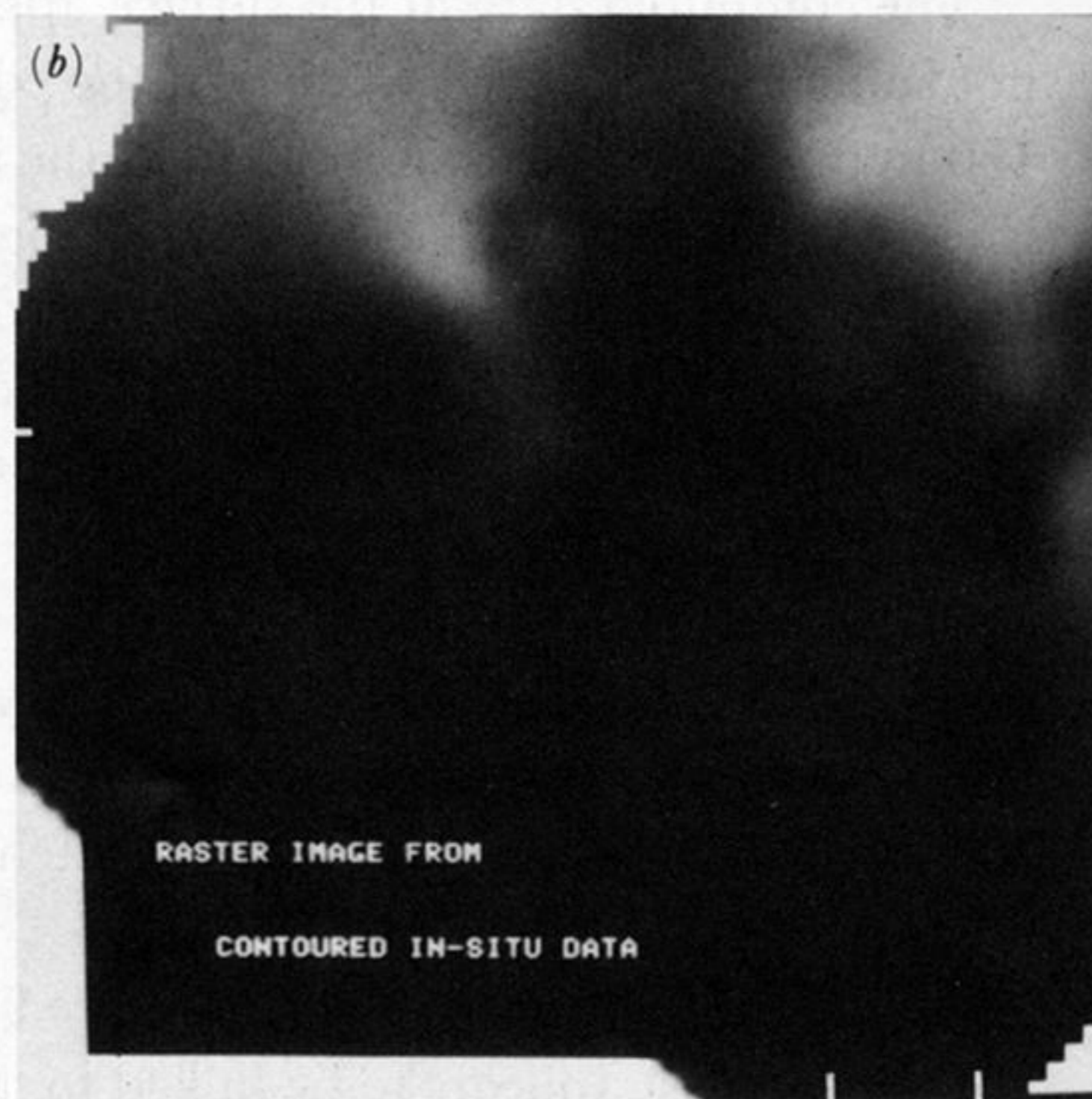
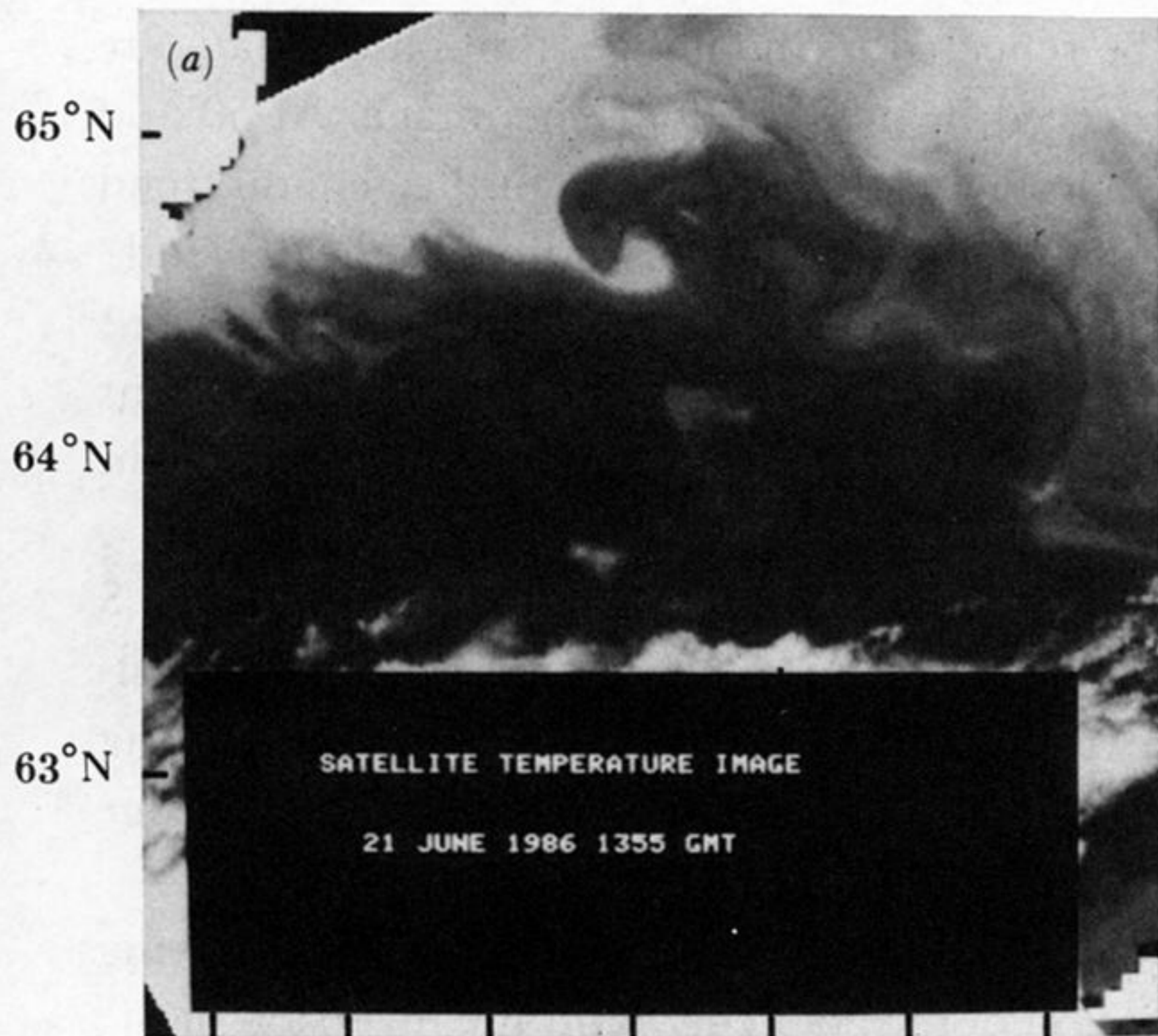


FIGURE 10. Satellite-derived and *in situ* measurements of sea-surface temperature presented in raster and vector mode. Both sets of contoured (vector) data show the general distribution of warm Atlantic water with the cooler Norwegian Sea water to the north. Comparison between overall grey level distribution in both raster images indicate the lighter shades in the *in situ* image corresponding to a lower temperature field.

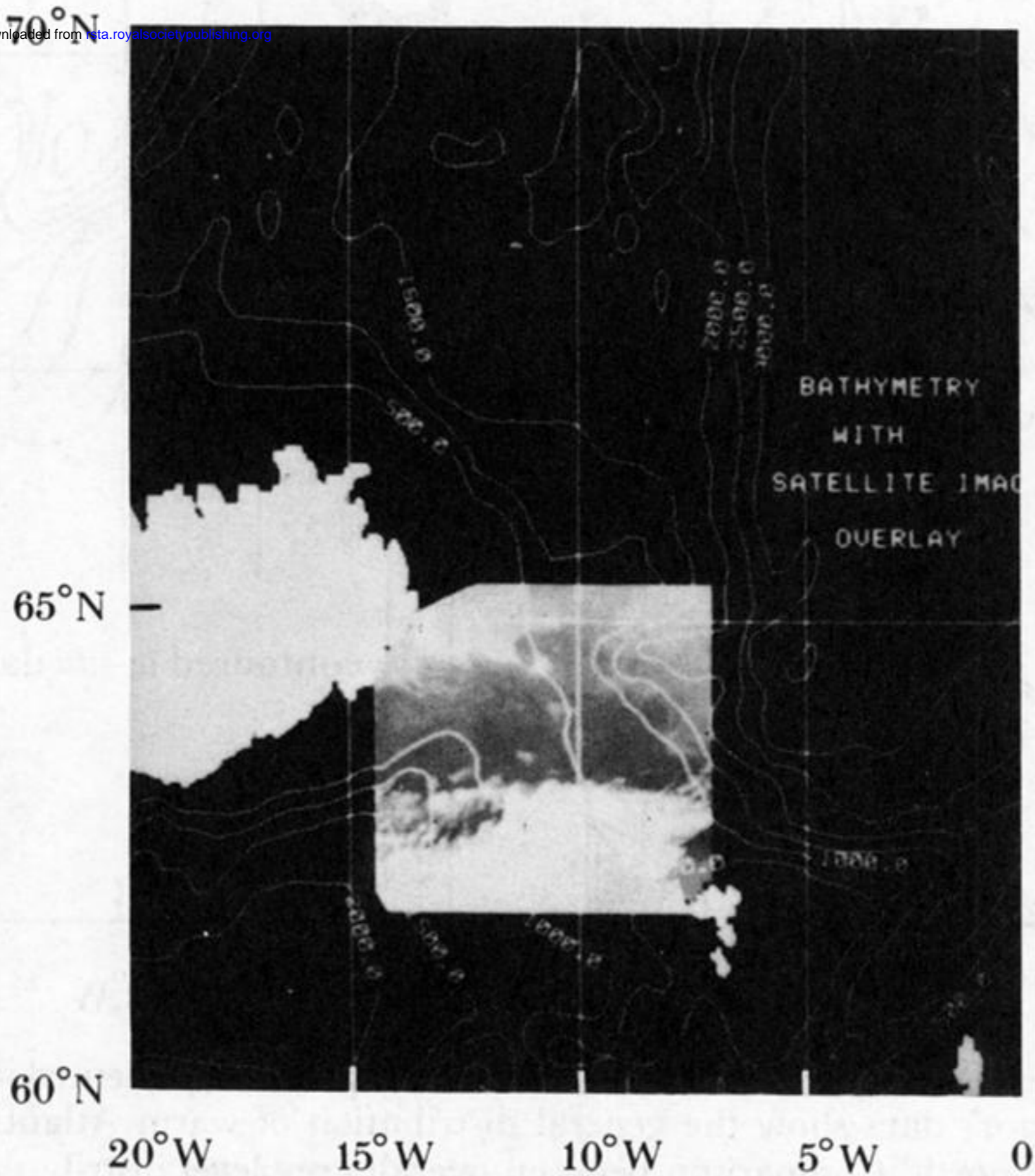


FIGURE 11. Satellite subimage overlaid on bathymetry contours. The spacing of the contours may be selected interactively by the user.

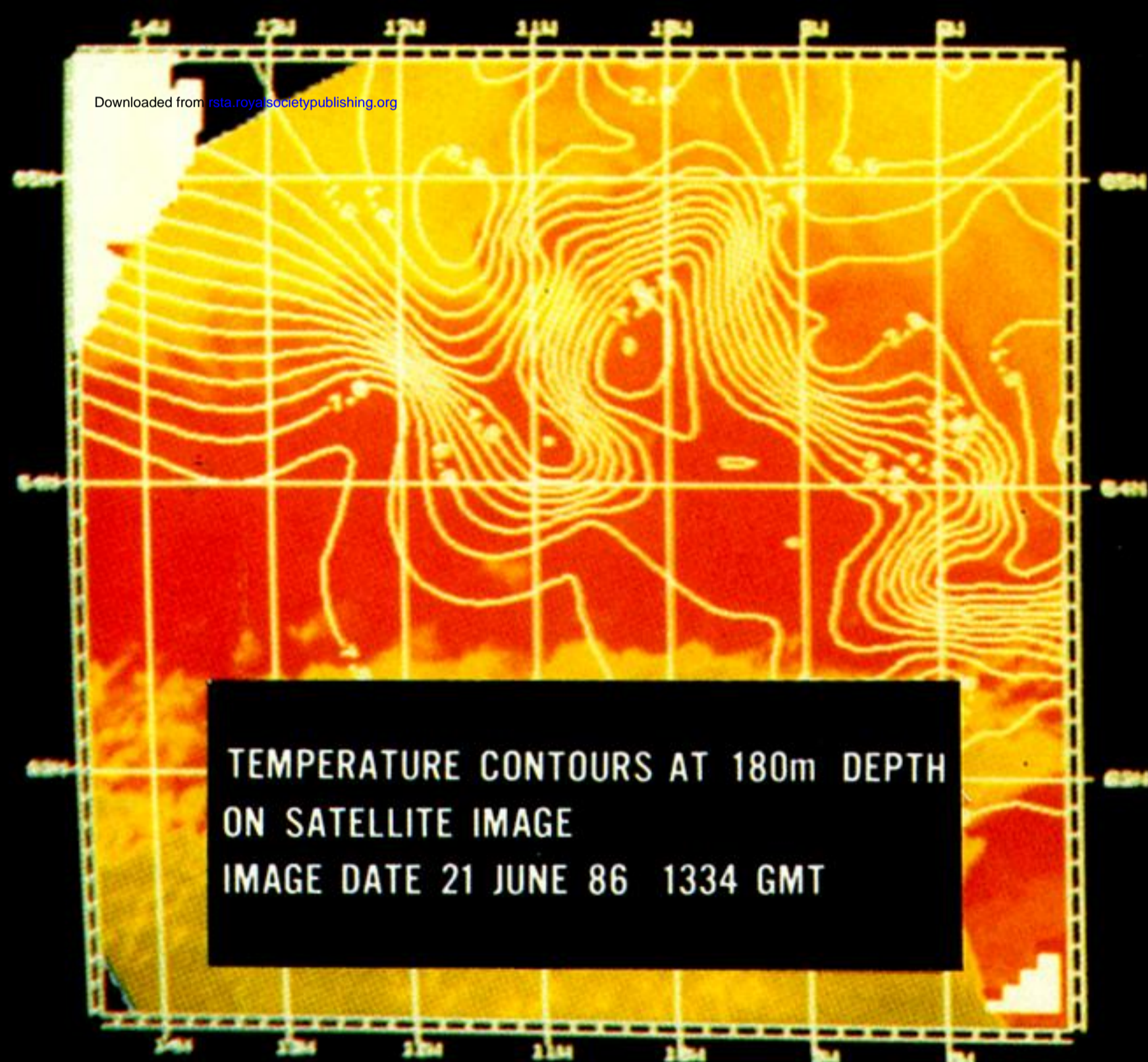
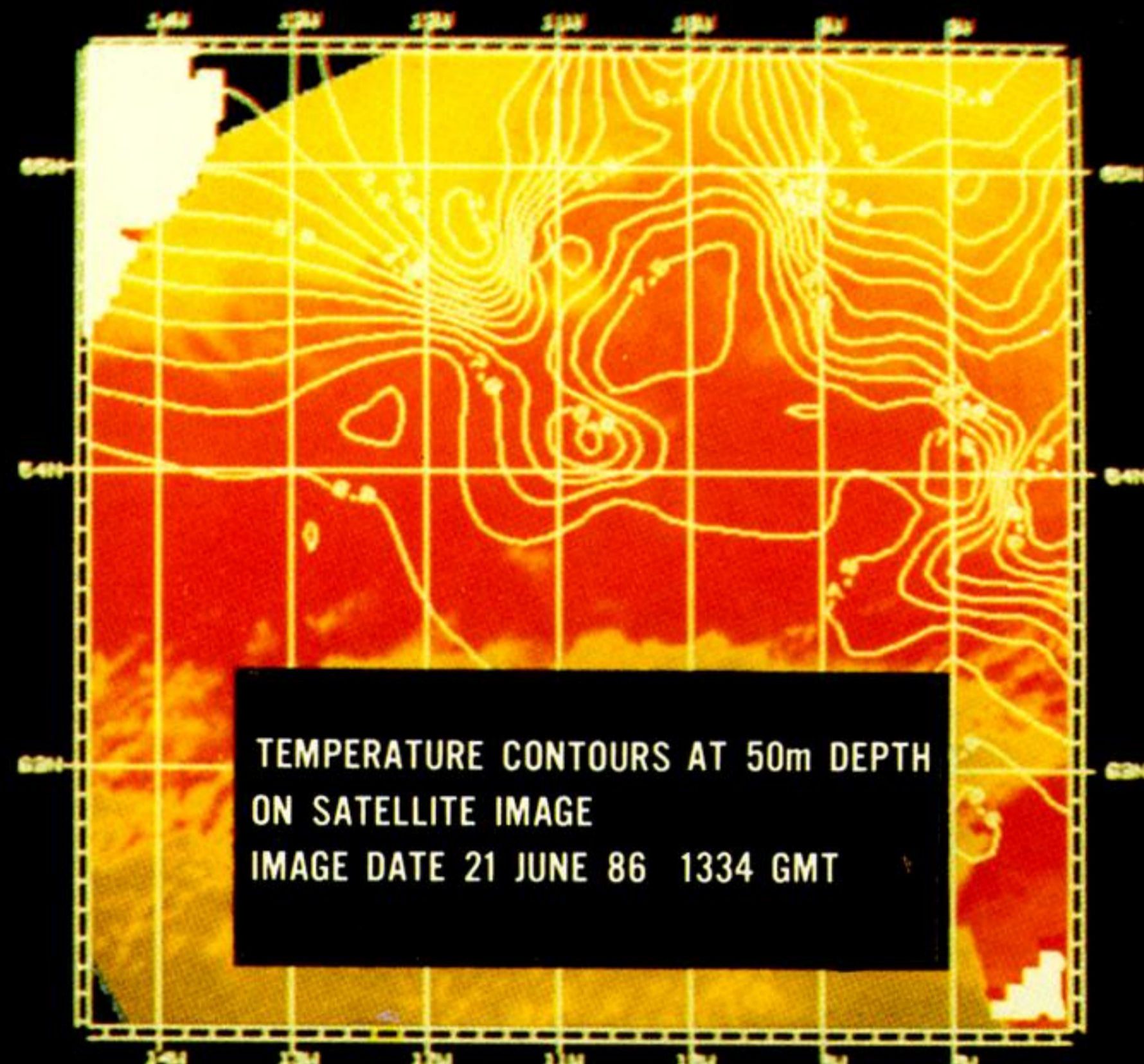
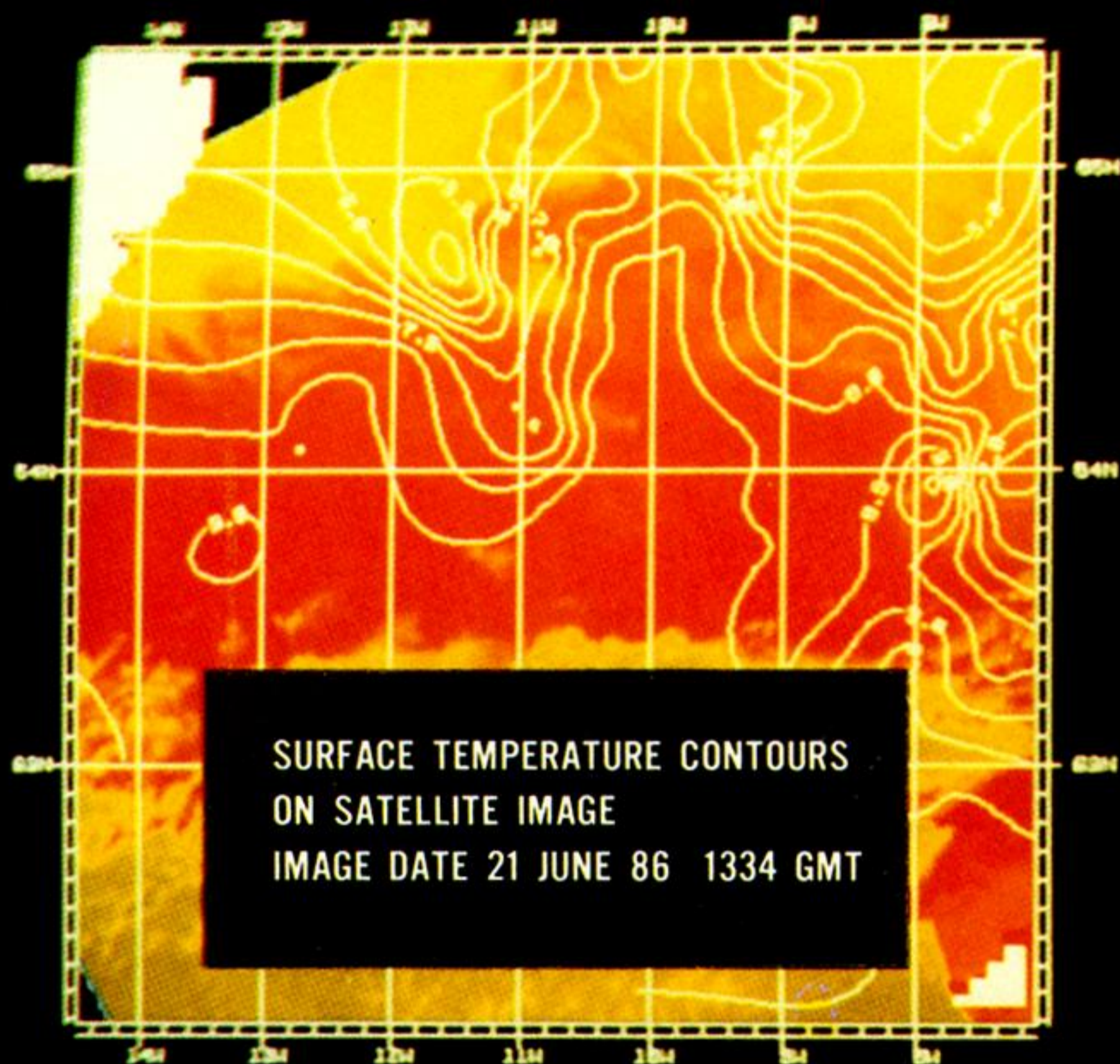


FIGURE 9. Contoured *in-situ* temperature data at significant depths of near-surface, 50m, 180m and 350m depth overlaid on the satellite subimage; an example of how *in-situ* data can be compared with accurately registered and atmospherically corrected satellite images.